Appl. Phys. B 79, 345–350 (2004)
DOI: 10.1007/s00340-004-1546-y

Applied Physics B
Lasers and Optics

M. GRAPINET[1,✉]
P. MATHEY[1]
S. ODOULOV[2]
D. RYTZ[3]

Phase diagrams for semilinear photorefractive coherent oscillator

[1] Laboratoire de Physique de l'Université de Bourgogne, UMR CNRS 5027, 9 avenue Alain Savary, 21078 Dijon Cedex, France
[2] Institute of Physics, National Academy of Sciences, 03650, Kiev-39, Ukraine
[3] Forschunginstitute für mineralische und metallische Werkstoffe, Edelsteine Edelmetalle GmbH, 55743 Idar-Oberstein, Germany

Received: 21 April 2004
Published online: 3 June 2004 •

ABSTRACT The sequence of optical phase transitions is considered for a photorefractive coherent oscillator with a conventional mirror and a four-wave mixing phase conjugate mirror. Analogous to phase transitions in solids, the phase diagrams are constructed and defined qualitatively as different states of a whole system (light-induced scattering below the threshold of oscillation, single-frequency oscillation, two-frequency oscillation, and multimode mirrorless oscillation). The attempt of experimental mapping of a phase diagram is presented for a coherent oscillator with Co-doped $BaTiO_3$.

PACS 42.65.Hw; 05.45.-a; 42.65.Pc; 42.65.Sf.

1 Introduction

In several recent publications the onset of oscillation in coherent oscillators based on nearly degenerate four–wave mixing was treated as an optical phase transition [1–5]. The state of the system below the threshold is considered as a disordered state (the crystal emits radiation with uncorrelated phases in a wide solid angle) while above the threshold the order is established (only one component of spatial spectrum is radiated and it collects the intensity which is much larger than the intensity of any particular scattered wave below the threshold). A strong modification occurs also in the spatial structure of the refractive index changes, below the threshold it looks like an irregular speckle-like pattern while above the threshold this random distribution transforms into a regular 3D index grating with a well defined single grating vector. These features suggest the scenario of an oscillation threshold to structural order–disorder phase transition in solid state physics that occurs with increasing temperature.

It is known that quite often one can also observe within the crystalline state, the other phase transitions when the crystal symmetry undergoes abrupt changes (e.g., ferroelectric phase transitions) or the crystal acquires a non–zero magnetic moment (ferromagnetic phase transitions). In a similar way the coherent oscillator can show critical changes in its operation mode, already above the threshold, for well developed oscillation. One example consists of the transition from an immobile refractive index grating to two gratings that are moving in opposite directions [6, 7]. This transition occurs when changing the pump intensity ratio or crystal coupling strength.

The purpose of this paper is to define the existence area for different characteristic modes of operation of a semilinear photorefractive coherent oscillator and to construct, in a way similar to how it is done in solid state physics, the diagrams of states (or 'phases'). Such phase diagrams help to deepen understanding of the analogy between phase transitions in optics and other fields of physics. They are useful also for conscious selection of the control parameters that ensure a desirable mode of operation.

Most of the theoretical dependencies follow from previously known calculations and they are assembled in a phase diagram for the first time. The experimental measurement of a phase diagram for $BaTiO_3$: Co is also presented.

2 Semilinear oscillator with two pump waves

The schematic representation of the coherent oscillator under consideration is shown in Fig. 1. The photorefractive crystal PRC with the nonlocal nonlinear response (index grating $\pi/2$-shifted with respect to the immobile light fringes) is pumped with two counterpropagating light waves. It serves as a phase conjugate mirror for any coherent incident beam with the same frequency and polarization and can form, together with the conventional mirror M a semilinear photorefractive oscillator, first described in the beginning of the 1980's by Feinberg et al. [8]. In Fig. 1, oscillation waves 4 and 3 develop from the light scattered from optical imperfections of the sample in the direction of cavity axis and are amplified via four wave mixing.

The oscillation waves are coupled to the pump waves either by the transmission or by the reflection refractive index gratings. To favour a specific type of coupling the two pump waves are chosen to be mutually incoherent with specially selected path differences. For transmission grating recording, e.g., the path of pump wave 1 is taken to be longer than the path of the wave 2 exactly for a doubled length of the cavity (the doubled distance $2L$ is between the crystal PRC and conventional mirror M). In this case, the light of pump wave 2 scattered in the direction of the conventional mirror M as wave 3 and reflected back to the crystal as wave 4, is mutually coherent to the light of pump wave 1, and is a prerequisite for the recording of an efficient transmission grating. In the oppo-

✉ Fax: +33-380/395-951, E-mail: pmathey@u-bourgogne.fr

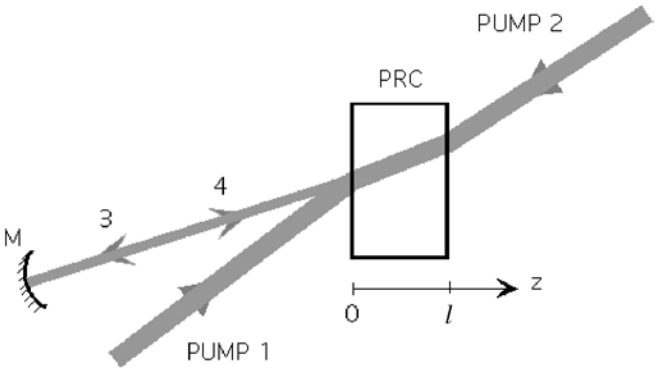

FIGURE 1 Semilinear photorefractive coherent oscillator with two counterpropagating pump waves. PRC is the photorefractive crystal, M is a conventional mirror

site symmetrical case when pump 2 propagates a longer way as compared to pump 1, the waves 4 and 2 become coherent and the reflection grating self-develops in the sample. A majority of the results reported in this paper are valid both in the case of only having either a transmission grating recording, or a reflection grating recording. In the following we will mainly discuss therefore, the transmission geometry. If not stated explicitly, the results can be taken as applicable also for the case of a reflection grating.

The necessary condition of oscillation in the considered geometry is in the self-reproduction of oscillating waves after one round trip in a semi-opened cavity. As one of the cavity mirrors is a phase conjugate mirror, the condition of self reproduction for the phase of the oscillation wave is met automatically for an arbitrary cavity length L. The condition of self reproduction for oscillation wave intensity imposes a condition that the wave intensity should remain the same after two consecutive reflections, once from the conventional mirror and then from the phase conjugate mirror, i.e.,

$$RR_{\mathrm{pc}} = 1, \tag{1}$$

where R and R_{pc} are the reflectivities of the conventional and phase conjugate mirrors, respectively. If supplemented by the dependence of R_{pc} on the main experimental parameters, (1) allows tracing of the threshold curve, i.e., to separate the area of parameters where the system is below the threshold from where oscillation occurs.

For frequency degenerate backward wave four wave mixing, the explicit expression for R_{pc} has been known for a long time [9]. The considered oscillator does not always generate only one single frequency that coincides with that of the pump waves, a bifurcation in the oscillation spectra occurs at a certain critical value of the parameters (such as coupling strength, beam ratio, or conventional mirror reflectivity). The problem is to find this frequency splitting from the self-consistent theory. Whenever this problem is solved one can define the above mentioned threshold curve and plot, in addition, the other curve that separates the areas of single-frequency and two-frequency oscillation.

At sufficiently high values of the coupling strength mirrorless oscillation may occur that can be regarded as one more state of the system. The propagation direction for this oscillation is not fixed by the cavity and it is always nondegenerate in frequency. Thus our phase diagrams should include a border that separates the area of mirrorless oscillation too.

Finally, it should be mentioned that the semilinear oscillator can also operate with only one of two pump waves [10], in particular with pump wave 2 as shown in Fig. 1. The onset of oscillation in this particular case requires a seeding radiation and features the properties of the first order phase transition [11, 12]. For a semilinear oscillator with one pump wave the single frequency oscillation is predicted [10]. The minimum coupling strength limit below which this type of oscillation is impossible is known from refs. [10, 11]. It is reasonable to mark in the phase diagrams,the regions where conventional oscillation with two pumps and oscillation with only one pump can compete.

In the next sections we recall the necessary solutions that allow design of the diagrams of state for semilinear coherent photorefractive oscillators, and to plot the diagrams themselves and compare them with the experimental data for a $BaTiO_3$ based oscillator.

3 Results of calculations

The oscillation is analysed within a plane wave approximation with a standard set of equations for slowly varying amplitudes A_i [10]

$$\begin{aligned}
\frac{\mathrm{d}A_1}{\mathrm{dz}} &= -\frac{\gamma}{I_0}\left(A_1A_4^* + A_2^*A_3\right)A_4 \\
\frac{\mathrm{d}A_2^*}{\mathrm{dz}} &= -\frac{\gamma}{I_0}\left(A_1A_4^* + A_2^*A_3\right)A_3^* \\
\frac{\mathrm{d}A_3^*}{\mathrm{dz}} &= \frac{\gamma}{I_0}\left(A_1A_4^* + A_2^*A_3\right)A_2 \\
\frac{\mathrm{d}A_4}{\mathrm{dz}} &= \frac{\gamma}{I_0}\left(A_1A_4^* + A_2^*A_3\right)A_1^*,
\end{aligned} \tag{2}$$

with the complex coupling constant

$$\gamma = \frac{\gamma_0}{1+(\Omega\tau)^2} + i\frac{\Omega\tau\gamma_0}{1+(\Omega\tau)^2} = \gamma'' + i\gamma', \tag{3}$$

that accounts for possible frequency detuning of the oscillation wave $\Omega = \omega_4 - \omega_1$ ($\omega_1 \equiv \omega_2$, $\omega_3 \equiv \omega_4$), τ being a space charge decay time. The photorefractive crystal itself possesses a purely nonlocal nonlinear response and its coupling constant γ_0 is therefore real.

The set of equations of (2) are written for transmission gratings and it should be underlined that two last equations coincide with those for the reflection geometry case if $A_1 \to A_3 \to A_2 \to A_4 \to A_1$. From this it can be concluded that in the undepleted pump approximation (when the two first equations of the set (1) are reduced to $\mathrm{d}A_1/\mathrm{d}z = \mathrm{d}A_2^*/dz = 0$) all the results of the theory for transmission gratings are also applicable for wave mixing with reflection gratings.

The intensity gain factor $\Gamma = 2\gamma''$ features a standard Lorentzian shape with the maximum at the frequency of the pump waves, $\Omega = 0$ (see (3)). The phase conjugate reflectivity R_{pc} may feature, however, either one or two maxima symmetric with respect to $\Omega = 0$ [13]. Figure 2 represents the spectra of reciprocal phase conjugate reflectivity $1/R_{\mathrm{pc}}$ for $\gamma_0\ell = -1$, -2.1, and -5, for the curves 1, 2, and 3, respectively (ℓ is the interaction length).

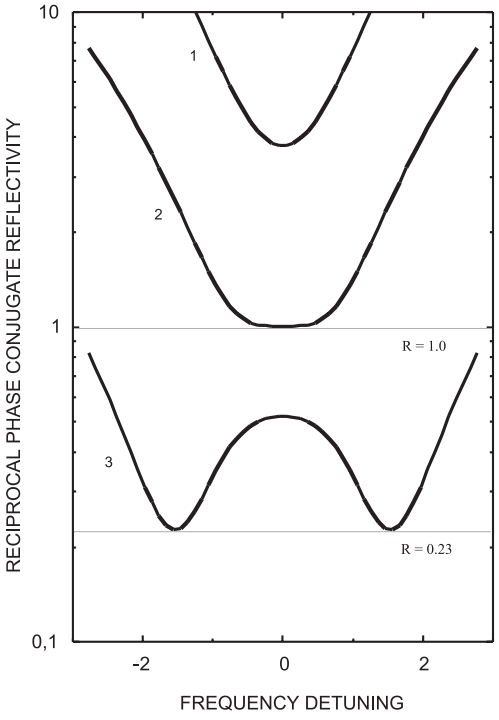

FIGURE 2 Threshold conditions of oscillation for the considered geometry, $1/R_{\rm pc} = R$. The oscillation is expected to appear at the frequencies $\Omega\tau$ that correspond to the minima of $1/R_{\rm pc}$

The horizontal lines show the reflectivity R of a conventional mirror. The oscillation occurs in the minima of $R_{\rm pc}^{-1}$ where the condition $R_{\rm pc}^{-1} = R$ is met (see (1)). One can see that for a moderate coupling strength $R_{\rm pc}^{-1}$ possesses only one minimum centered at $\Omega = 0$ while for $\gamma_0\ell < -2.1$ the two symmetric minima appear. Note that such a form of presentation of the threshold condition remains the same as the transition from one-minimum to two-minima dependence for free energy in the theory of phase transitions [14].

3.1 *Threshold of oscillation in the cavity*

Taking into account that at the threshold the phase conjugate reflectivity is

$$R_{\rm pc} = \frac{\sinh^2\left(\frac{\gamma''\ell}{2}\right) + \sin^2\left(\frac{\gamma'\ell}{2}\right)}{\cosh^2\left(\frac{\gamma''\ell - \ln r}{2}\right) - \sin^2\left(\frac{\gamma'\ell}{2}\right)}, \tag{4}$$

and that oscillation should occur at the frequencies that ensure the largest possible phase conjugate reflectivity

$$\frac{{\rm d}\,R_{\rm pc}}{{\rm d}\Omega} = 0, \tag{5}$$

one can arrive at the equation

$$\frac{{\rm d}\gamma''\ell}{{\rm d}\Omega}\left[-2\sin^2\left(\frac{\gamma'\ell}{2}\right)\sinh\left(\gamma''\ell - \frac{\ln r}{2}\right) + 2\sinh\left(\frac{\gamma''\ell}{2}\right)\cosh\left(\frac{\gamma''\ell - \ln r}{2}\right)\right] = -\frac{{\rm d}\gamma'\ell}{{\rm d}\Omega}\sin\left(\gamma'\ell\right)\cosh\left(\gamma''\ell - \frac{\ln r}{2}\right), \tag{6}$$

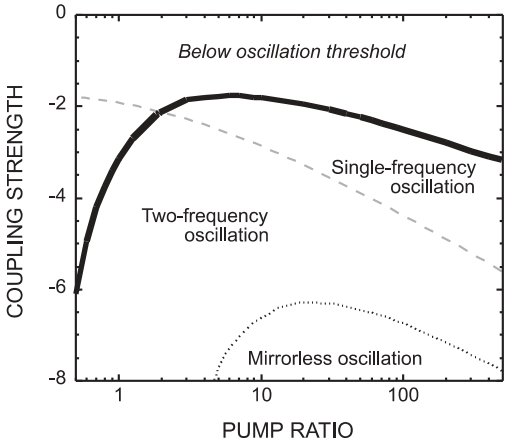

FIGURE 3 Phase diagram for considered semilinear oscillator with $R = 1$. The thick *solid line* defines the threshold condition; the gray *dashed line* marks the bifurcation of single-frequency into two-frequency oscillation, and the *dotted line* separates the area where mirrorless oscillation occurs

that allows, when solved numerically together with (1), the calculation of the threshold condition of oscillation. The dependence of the threshold coupling strength $(\gamma_0\ell)_{\rm th}$ on pump ratio r is shown in Fig. 3 by the solid line. It should be noted that the analytic solution is also available for those r values for which the oscillation occurs with a single frequency [7]:

$$(\gamma_0\ell)_{\rm th} = \ln\frac{\sqrt{r\,R} - 1}{\sqrt{r}\left(\sqrt{R} + \sqrt{r}\right)}. \tag{7}$$

3.2 *Threshold of bifurcation*

By definition bifurcation occurs in the vicinity of the extremum when the curvature of $R_{\rm pc}\ (\Omega)$ changes its sign

$$\frac{{\rm d}^2 R_{\rm pc}}{{\rm d}\Omega^2} = 0. \tag{8}$$

Equations (1), (4), (5), and (8), when solved together, lead to the relationship

$$r = \frac{\gamma_0\ell\,\exp\left(\gamma_0\ell\right) + 2\left[1 - \exp\left(\gamma_0\ell\right)\right]}{-\gamma_0\ell\,\exp\left(-\gamma_0\ell\right) + 2\left[1 - \exp\left(\gamma_0\ell\right)\right]}, \tag{9}$$

that defines the border line between the area of single-frequency oscillation and two-frequency oscillation. It is shown by dashes in Fig. 3.

3.3 *Threshold of mirrorless oscillation*

This threshold dependence can be derived analytically from (1) and (4) by imposing $R_{\rm pc} = \infty$, i.e. $R = 0$, which means that the cavity is not closed with a conventional cavity mirror. The relevant equation reads as:

$$(\gamma_0\ell)_{\rm th}^{\rm ml} = -\ln r\,\left[1 + (\pi/\ln r)^2\right], \tag{10}$$

where the superscript ml at the coupling strength denotes mirrorless oscillation. This dependence is plotted in Fig. 3 by dots.

3.4 *Thershold of oscillation with only one pump wave*

The threshold has been detailed for this case by Cronin-Golomb et al. [10]. In a formal way the threshold of oscillation is infinitely large in this case but if initially seeded, steady state oscillation is self-supported. The relevant expression for the minimum coupling strength at which oscillation still exists is given by:

$$(\gamma_0\ell)_{\text{th}} = \sqrt{1+R}\ln\left[\frac{\sqrt{1+R}-1}{\sqrt{1+R}+1}\right]. \tag{11}$$

It depends on R and corresponds to $r = \infty$ (no backward pump is needed). Equation (11) is derived for strictly degenerate four-wave mixing.

According to (11) the smallest threshold that corresponds to $R = 1$ is $(\gamma_0\ell)_{\text{th}} = -2.49$. This means that for $(\gamma_0\ell)_{\text{th}} < -2.49$ such an oscillation can compete, in principle, with that which is due to the presence of two pump waves.

It is important to underline the fact that oscillation with one pump wave cannot occur in the case of the reflection grating recording.

4 Experimental

To check the predictions described above requires studying of the oscillation in a semilinear cavity with a Co-doped $BaTiO_3$ sample (Fig. 4). Ar^+-laser light (0.51 μm, about 200 mW in single transverse mode) is used to pump the crystal. A conventional spherical cavity mirror M_c closes the cavity. The path difference of the two pump waves is large compared to the laser beam coherence length (a few cm). It is chosen to ensure mutual coherence for pump wave 1 and wave 4 that is reflected back to the sample by the mirror M. A small aperture (0.5 mm) is put inside the cavity at 5 cm from the conventional mirror. A Faraday isolator is placed at the Ar^+-laser output mirror to prevent undesirable feedback to the pump laser from the coherent oscillator.

The pump waves 1 and 2 make angles of 167.7° and 12.3° with regard to the spontaneous polarization axis (Z–axis) inside the sample. The position of the conventional mirror ensures respective angles of 170.6° and 9.4° between the sample polar axis and oscillation waves 3 and 4, also inside the sample. This geometry, in accordance with the calculations of Feinman et al. [15], is close to optimal for the largest possible gain from the transmission grating in $BaTiO_3$.

The pump waves are loosely focused inside the sample with a lens of 100 cm focal length. A half-wave phase retarder $\lambda/2$ and a polarizer P allow for a reduction of the pump 1 intensity while keeping the intensity of pump 2 constant.

The oscillation intensity is measured with the detector PD that collects the beam reflected from the sample face; therefore $I_3(0)$ is monitored. Depending on the particular value of the pump ratio the oscillation dynamics at saturation is either smooth or features periodic variation what proves the existence of two temporal frequencies in the oscillation spectrum. Thus, two qualitatively different operation modes can be revealed and the bifurcation points can be found.

As the coupling strength in $BaTiO_3$ is independent of pump intensity it was controlled by changing the polarization of the two pump waves. The identical $\lambda/2$ phase retarders were placed in each pump beam before the sample and they were both rotated to the same angle α. The coupling strength was therefore decreased to

$$\gamma\ell = \gamma\ell_0\cos^2 2\alpha. \tag{12}$$

In the experiment, at first α is set to zero and two-frequency oscillation is observed. Than α is increased, step by step, to detect the value at which the two frequencies collapse into one. In this way a critical bifurcation value of coupling strength is measured. With α increasing further we come to the second critical value of coupling strength that marks the disappearance of oscillation (threshold of oscillation). Such a procedure is repeated for different pump ratios. The results are shown in Fig. 5.

In the same figure the calculated dependencies are shown. Two fitting parameters are used here. One is the unknown effective reflectivity R_{eff} of the conventional mirror that accounts for all kinds of cavity losses. The other one is the initial coupling strength of the crystal. The quantities extracted from the fit are $R_{\text{eff}} = 0.25$ and $\gamma_0\ell \approx -3.8$.

The value for R_{eff} looks reasonable if one takes into account Fresnel reflections from sample faces, sample absorp-

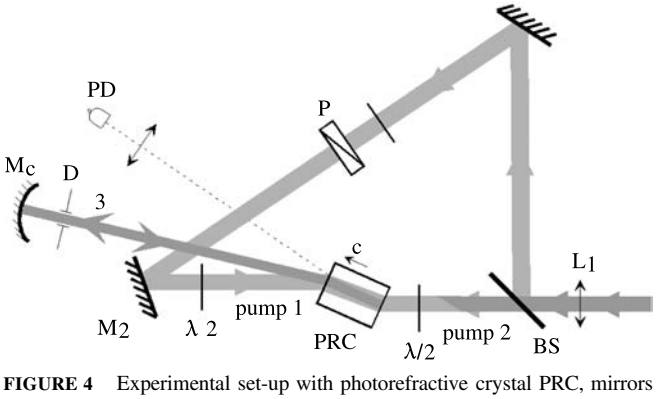

FIGURE 4 Experimental set-up with photorefractive crystal PRC, mirrors M, lenses L, half wave phase retarders, polarizer P, aperture D, and photodetector PD

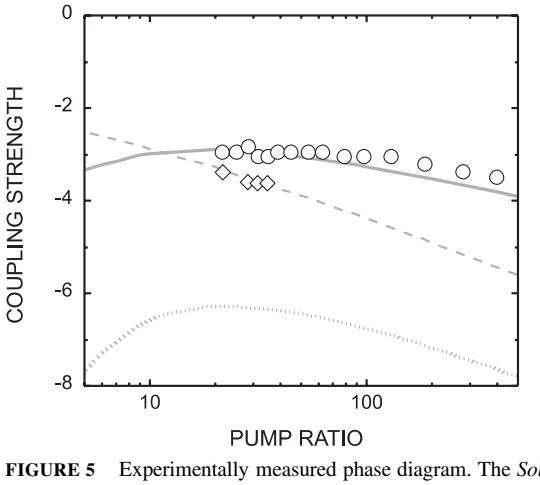

FIGURE 5 Experimentally measured phase diagram. The *Solid line* marks the threshold condition for $R_{\text{eff}} = 0.25$, the *dashed line* defines bifurcation in the oscillation spectrum, and the *dotted line* indicates the possible onset of mirrorless oscillation

tion, diffraction losses because of a small diaphragm, etc. It is close to that evaluated in our previous experiments on frequency splitting [6].

The value for $\gamma_0\ell$ is nearly one half of the initial coupling strength measured in for this sample a few years ago [6, 7]. This can be a consequence of the appearance of misaligned ferroelectric domains in the bulk after extensive use in optical experiments.

It should be noted that close values for $\gamma_0\ell$ and R_{eff} were also extracted from the independent check, from the range of oscillation existence in the pump ratio. Exactly at the threshold, the coupling strength is related to the pump ratio r via (7). In the degenerate case, the oscillation occurs within a certain range of pump ratio, with two limiting values r_1 and r_2 that satisfy the relation :

$$(\gamma_0\ell)_{\text{th}} = \ln\frac{\sqrt{R_{\text{eff}}r_1}-1}{\sqrt{r_1}(\sqrt{R_{\text{eff}}}+\sqrt{r_1})} = \ln\frac{\sqrt{R_{\text{eff}}r_2}-1}{\sqrt{r_2}(\sqrt{R_{\text{eff}}}+\sqrt{r_2})}. \tag{13}$$

From the above equality, the reflectivity R_{eff} and the coupling strength can be written as:

$$R_{\text{eff}} = \left[\frac{\sqrt{r_1}+\sqrt{r_2}}{\sqrt{r_1r_2}-1}\right]^2, \tag{14}$$

$$(\gamma_0\ell)_{\text{th}} = -\ln\sqrt{r_1r_2}\,. \tag{15}$$

The numerical values of $(\gamma_0\ell)_{\text{th}} \approx -3.9$ and $R_{\text{eff}} \approx 0.3$ deduced from the measured pump ratio dependence of the oscillation intensity, are in close agreement with the values extracted from the fit shown in Fig. 5.

5 Supplementary phase diagrams

There is one more control parameter apart from the coupling strength and pump ratio considered above. It is the reflectivity of a conventional mirror. A 3D phase diagram can be constructed, or two additional 2D diagrams may be plotted.

Figure 6 shows a phase diagram of variable pump ratios against conventional mirror reflectivity values. The threshold curve that separates the area where oscillation can exist with a crystal of $\gamma_0\ell \approx -3$, is shown by the thick solid line. For a crystal with smaller coupling strength, $\gamma_0\ell \approx -2$, a higher reflectivity of the conventional mirror is necessary to get oscillation (black dotted curve). These curves are calculated numerically by solving (1), (5), and (6) with the given values of $\gamma_0\ell$.

The gray dashed line separates the area of single frequency oscillation and two-frequency oscillation. The relation linking r_{cr} and the reflectivity R of the conventional mirror is deduced from (1) and (8) with $\Omega = 0$. For $\Omega = 0$, (8) gives the result indicated in (3), and (1) ($RR_{\text{pc}} = 1$) leads to (7). Rewriting this expression for $\gamma_0\ell$ in (9), yields:

$$\ln\frac{\sqrt{r_{\text{cr}}}(\sqrt{R}+\sqrt{r_{\text{cr}}})}{\sqrt{Rr_{\text{cr}}}-1} = \frac{2(1+r_{\text{cr}})\sqrt{R}}{(1+R)\sqrt{r_{\text{cr}}}}. \tag{16}$$

The dependence of R on r_{cr} in Fig. 6 is calculated from (16).

The third phase diagram is plotted with coupling strength and conventional mirror reflectivity as the variables. The threshold curves are calculated numerically from the equations (1), (5), (6) while the bifurcation curve is deduced from the common solution of (9) and (16).

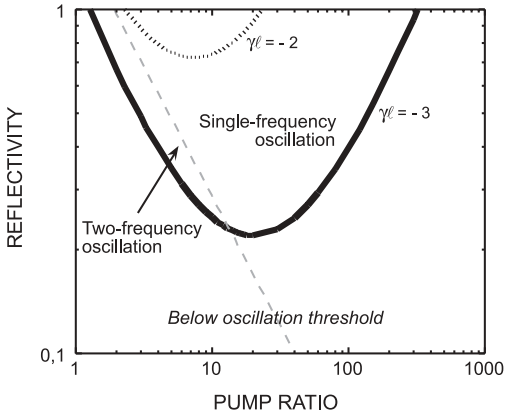

FIGURE 6 Phase diagram with control parameters R and r. Two *threshold lines* are shown, one for coupling strength $\gamma_0\ell = -3$ (thick *solid line*), and the other for $\gamma_0\ell = -2$ (*dotted line*). The gray *dashed line* marks the bifurcation in the temporal frequency spectra

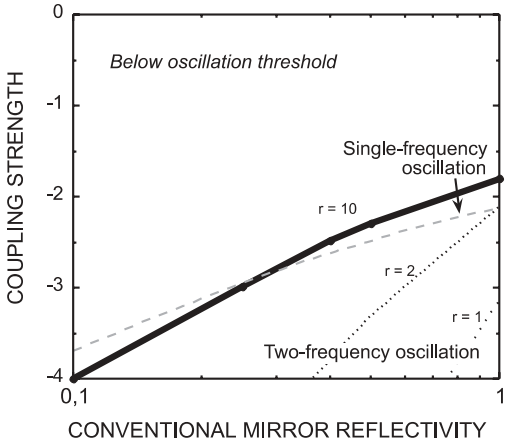

FIGURE 7 Phase diagram with control parameters $\gamma_0\ell$ and R. Three threshold lines are shown, for the pump ratio $r = 10$ (*thick solid line*), for $r = 2$ (*dotted line*), and for $r = 1$ (*rare dots*). The gray *dashed line* marks bifurcation in the temporal frequency spectra

Here again we can see that on increasing the coupling strength, the oscillation can start from a single frequency that bifurcates further into two frequencies, or double-frequency oscillation appears at the threshold. The range of existence of single-frequency oscillation becomes smaller with a decreasing pump ratio. For $r = 1$ single-frequency oscillation does not occur at all [7].

Until now we considered only oscillators with an empty cavity. This is not however always the case. An amplifier may be placed between the conventional mirror and phase conjugate mirror so that the effective reflectivity of the conventional mirror becomes larger than unity, $R > 1$. This hybrid oscillator that combines the gain from conventional laser medium and that from four-wave mixing is of particular interest because of its potential ability to generate aberration-free beams with a small divergence [10, 16, 17].

The use of a mirror with a reflectivity higher than unity makes less rigid the requirements of the coupling strength, so the threshold coupling strength becomes smaller. The threshold curve in Fig. 3 goes up, therefore decreasing the area below the oscillation threshold. The amplifying mirror also al-

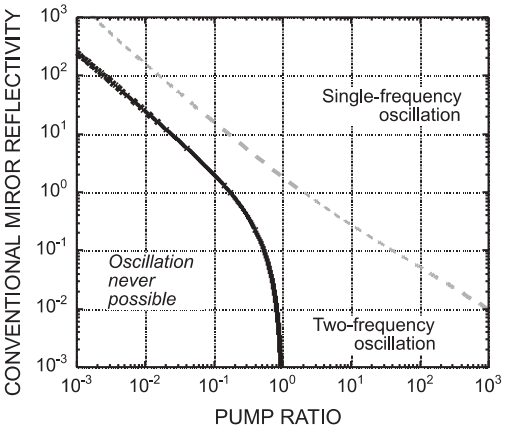

FIGURE 8 Phase diagram with control parameters R and r. The *thick solid line* separates the area where oscillation can exist. The *gray dashed line* marks bifurcation in the temporal frequency spectra

lows for oscillation over an extended range of pump ratios, especially for $r < 1$. At the same time even with $R > 1$ there are some combinations of parameters where oscillation can never be achieved. This is illustrated with the extended range $R - r$ phase diagram shown in Fig. 8.

Below the thick threshold line, for example, the oscillation cannot occur whatever the coupling strength $\gamma_0\ell$, of the crystal. If the pump ratio r is larger than 1 the oscillation with two pump waves may occur even for $R = 0$ (mirrorless oscillation) [7]. This oscillation is always nondegenerate in frequency. For $\gamma_0\ell < -2.49$ oscillation becomes possible for $r \to \infty$, i.e., with only one pump wave, and its frequency coincides with that of the pump waves.

Of course, for moderate values of coupling strengths $\gamma_0\ell$, the threshold curves are not as that shown in Fig. 8 for $\gamma_0\ell \to -\infty$, and the area where oscillation occurs becomes smaller. Two particular threshold curves are shown in Fig. 6 for $\gamma_0\ell = -2$ and $\gamma_0\ell = -3$. Thus the phase diagram presented in Fig. 8 defines the areas where single-frequency oscillation and/or two-frequency oscillation can exist in principle. For any point below the threshold curve, oscillation is impossible. Above this curve oscillation may or may not exist. However, depending on particular values of r and R, it will always be either single-frequency oscillation or two-frequency oscillation.

6 Conclusions

Three types of phase diagrams are constructed for the optical phase transitions in a semilinear photorefractive oscillator with two pump waves. The coupling strength of the sample, pump intensity ratio, and reflectivity of a conventional mirror, are chosen as the control parameters, while the normalized oscillation intensity and normalized frequency detuning serve as the order parameters. Several new relations are derived from the solution of the standard set of equations (2), that are necessary to define the borders of 'phases' in phase diagrams.

It should be stressed that all curves that separate different 'phases' represent the respective threshold values, i.e., correspond to zero intensity of the oscillation wave. This approach is obviously true for the second order phase transitions, as for example, with the onset of oscillation with an increasing coupling strength [5]. It may happen that the transitions with other control parameters feature subcritical bifurcations and it will be necessary to modify the notion of the threshold. Investigations in this direction are now in progress.

The experimental data for $BaTiO_3$ based coherent oscillators are in reasonable agreement with the results of calculation.

ACKNOWLEDGEMENTS This work was supported in part by Alexander von Humboldt Stiftung via a research award attributed to S. Odoulov.

REFERENCES

1 D. Engin, S. Orlov, M. Segev, G. Valley, A. Yariv: Phys. Rev. Lett. **74**, 1743 (1995)
2 F.T. Arecchi, G. Giacomelli, P.L. Ramazza, S. Residori: Phys. Rev. Lett. **65**, 2531 (1990); **67**, 3749 (1991)
3 S. Odoulov, M. Goul'kov, O. Shinkarenko: Phys. Rev. Lett: **83**, 3637 (1999)
4 M. Goul'kov, O. Shinkarenko, S. Odoulov, E. Krätzig, R. Pankrath: Appl. Phys. B **72**, 187 (2001)
5 P. Mathey, P. Jullien, S. Odoulov, O. Shinkarenko: J. Opt. Soc. Am. B **19**, 405 (2001)
6 P. Mathey, S. Odoulov, D. Rytz: Phys. Rev. Lett. **89**, 053 901 (2002)
7 P. Mathey, S. Odoulov, D. Rytz: J. Opt. Soc. Am. B **19**, 2967 (2002)
8 J. Feinberg, R. Hellwarth: Opt. Lett. **5**, 519 (1980)
9 M. Cronin-Golomb, B. Fischer, J.O. White, A. Yariv: Opt. Lett. **7**, 313 (1982)
10 M. Cronin-Golomb, B. Fischer, J.O. White, A. Yariv: IEEE J. Quant. Elect. **QE-20**, 12 (1984)
11 S. Keung-Kwong, M. Cronin-Golomb, A. Yariv: Appl. Phys. Lett. **45**, 1016 (1984)
12 A. Zozulya: IEEE J. Quant. Elect. **QE-29**, 538 (1993)
13 K.R. McDonald, J. Feinberg: Phys. Rev. Lett. **55**, 821 (1985)
14 R. Kubo: *Statistical mechanics* (North-Holland, Amsterdam 1965)
15 Y. Feinman, E. Klancnik, S.H. Lee: Opt. Eng. **25**, 228 (1986)
16 A. Bagan, V. Gerasimov, A. Golyanov, E. Ogluzdin, V. Sugrobov, I. Rubtsova, A. Khyzhnjak: Sov. J. Quant. Elect. **17**, 49 (1990)
17 D.A. Rockwell: *Application of phase conjugation to high power lasers*, in "Optical Phase Conjugation, M. Grower (ed.), P. Proch, (Springer Verlag, Berlin, Heidelberg 1994) pp. 228–313